The Astrophysical Journal Letters, 836:L28 (5pp), 2017 February 20 https://doi.org/10.3847/2041-8213/aa5eae

A Common Origin of Magnetism from Planets to White Dwarfs

Jordi Isern[1,2], Enrique García-Berro[2,3], Baybars Külebi[1,2], and Pablo Lorén-Aguilar[4]

[1] Institut de Ciències de l'Espai (CSIC), Campus UAB, 08193 Cerdanyola, Spain

[2] Institut d'Estudis Espacials de Catalunya, Ed. Nexus-201, c/Gran Capità 2-4, E-08034 Barcelona, Spain

[3] Departament de Física, Universitat Politècnica de Catalunya, c/Esteve Terrades, 5, E-08860 Castelldefels, Spain

[4] School of Physics, University of Exeter, Stocker Road, Exeter EX4 4QL, UK

Received 2016 October 20; revised 2017 January 21; accepted 2017 February 4; published 2017 February 17

Abstract

Isolated magnetic white dwarfs have field strengths ranging from kilogauss to gigagauss. However, the origin of the magnetic field has not been hitherto elucidated. Whether these fields are fossil, hence the remnants of original weak magnetic fields amplified during the course of the evolution of their progenitor stars, or are the result of binary interactions, or, finally, they are produced by other internal physical mechanisms during the cooling of the white dwarf itself, remains a mystery. At sufficiently low temperatures, white dwarfs crystallize. Upon solidification, phase separation of its main constituents, ^{12}C and ^{16}O, and of the impurities left by previous evolution occurs. This process leads to the formation of a Rayleigh–Taylor unstable liquid mantle on top of a solid core. This convective region, as it occurs in solar system planets like the Earth and Jupiter, can produce a dynamo able to yield magnetic fields of strengths of up to 0.1 MG, thus providing a mechanism that could explain magnetism in single white dwarfs.

Key words: stars: interiors – stars: magnetic field – white dwarfs

1. Introduction

White dwarfs are the most common end-point of stellar evolution (Althaus et al. 2010). Some of them have measurable magnetic fields with strengths ranging from 10^3 to 10^9 G (Ferrario et al. 2015). The incidence of magnetism is a matter of debate. In volume-limited surveys—those that select stars within a maximum distance from the Sun—the incidence of magnetism is ∼20% (Kawka et al. 2007; Giammichele et al. 2012; Sion et al. 2014), while for magnitude-limited surveys—those selecting stars brighter than a given apparent magnitude—it is ∼8% (Liebert et al. 2003; Kepler et al. 2013, 2016). Nevertheless, because a population of white dwarfs with magnetic fields weaker than ∼1 kG may exist, the fraction of magnetic white dwarfs could be larger (Koester et al. 2011; Kawka & Vennes 2012; Ferrario et al. 2015). Observations also suggest (Valyavin & Fabrika 1999; Liebert et al. 2003; Kawka & Vennes 2014; Sion et al. 2014; Valyavin et al. 2014; Hollands et al. 2015) that the fraction of white dwarfs with strong magnetic fields is larger at low effective temperatures. This could indicate that magnetic fields are amplified during the evolution of white dwarfs. This interpretation, however, has been questioned (Ferrario et al. 2015) because apparently there is no clear correlation between the strength of the magnetic field and the luminosity, except for low magnetic field ($B \lesssim 0.1$ MG) white dwarfs. Interestingly enough, the observed paucity of white dwarfs with magnetic fields between 0.1 and 1 MG (Koester et al. 2011; Kawka & Vennes 2012) suggests a bimodal distribution (Ferrario et al. 2015).

The origin of magnetic white dwarfs remains unknown, and up to now three scenarios have been proposed. Within the first of them, white dwarf magnetic fields are the fossil remnants of those of their progenitors. Thus, the progenitors of magnetic white dwarfs could be main-sequence Ap/Bp stars (Angel et al. 1981; Wickramasinghe & Ferrario 2005), or could be the result of field amplification during the helium-burning phase (Levy & Rose 1974). Within the second scenario, magnetic white dwarfs are the result of the evolution of binary systems. In this case the magnetic field is amplified by a dynamo that operates either during the common envelope phase (Tout et al. 2008; Nordhaus et al. 2011) or in the hot corona produced during the merger of two white dwarfs (García-Berro et al. 2012). A difficulty of these two scenarios is that detailed population synthesis studies cannot reproduce the number of stars observationally found (Ferrario et al. 2015). Finally, within the third scenario the field is generated in the outer convective envelope that is formed during the evolution of single white dwarfs. However, theoretical calculations show that the strength of the resulting field is $\lesssim$0.01 MG (Fontaine et al. 1973; Tremblay et al. 2015), well below the observed magnetic fields, so a more efficient mechanism should be invoked.

The evolution of white dwarfs can be described as a simple gravothermal process (Althaus et al. 2010). The core of the vast majority of white dwarfs is made of a completely ionized mixture of ^{12}C and ^{16}O, and some minor chemical species like ^{22}Ne and ^{56}Fe. During their evolution, two physical processes modify the internal chemical profiles of white dwarfs. The first one is gravitational settling of neutron-rich species in the liquid phase (Bravo et al. 1992; Bildsten & Hall 2001; García-Berro et al. 2010; Camisassa et al. 2016), which occurs at moderately high luminosities. The second one is phase separation upon crystallization (Isern et al. 1997, 2000; García-Berro et al. 2010), and takes place at lower luminosities. In both cases, the energy involved is large, $\sim 2 \times 10^{46}$ erg.

For the sake of simplicity, here we will only consider white dwarfs made of ^{12}C and ^{16}O. The phase diagram of the carbon–oxygen mixture is of the spindle form (Segretain & Chabrier 1993; Horowitz et al. 2010). Since the solid phase is oxygen-rich, hence denser than the liquid phase, when white dwarfs crystallize it settles down, while the carbon-rich liquid left behind is redistributed by Rayleigh–Taylor instabilities (Isern et al. 1997, 2000). This configuration, a solid core surrounded by a convective mantle driven by compositional

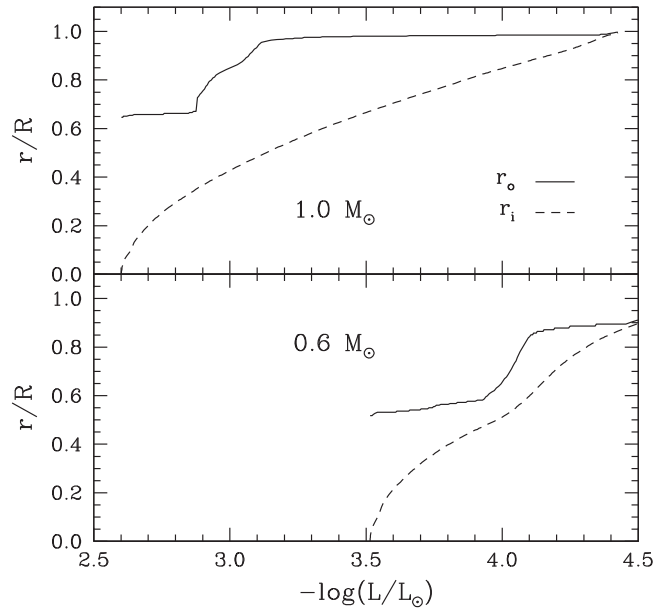

Figure 1. Evolution of the inner and outer radii of the convective mantle of a carbon–oxygen white dwarf as a function of the luminosity. The upper and lower panels correspond to white dwarfs with masses 1.0 and 0.6 $M_\odot$, respectively. Their respective total radii are $R = 4.7 \times 10^8$ and 7.5×10^8 cm.

buoyancy is similar to that found in the core of the Earth, where the light element release associated with the inner core growth is a primary driver of the dynamo (Lister & Buffet 1995). Given this analogy, in this Letter, we analyze if the convective mantle of crystallizing white dwarfs can produce magnetic fields of the observed strengths.

2. The Stellar Dynamo

For a typical white dwarf of mass $\simeq$0.61 $M_\odot$ solidification starts at $\log(L/L_\odot) \simeq -3.5$, whereas for a massive one of 1.0 $M_\odot$ crystallization sets in at $\simeq -2.6$. At this point of the evolution the temperatures of their nearly isothermal cores are, respectively, $\log T_c$ (K) = 6.3 and 6.6, whereas their central densities are $\log \rho_c$ (g cm^{-3}) = 6.6 and 7.5 (Salaris et al. 2010). For the sake of conciseness, and unless specified otherwise, here we will only discuss the case of the heavier white dwarf, since it is observationally found that magnetic white dwarfs are more massive than usual (Ferrario et al. 2015).

As can be seen in Figure 1, for a 1.0 $M_\odot$ white dwarf, when solidification starts the Rayleigh–Taylor unstable region encompasses a large fraction of the radius of the star. This also holds for the 0.6 $M_\odot$ model star. As the 1.0 $M_\odot$ white dwarf cools, the outer edge of the convective mantle barely moves, while the inner edge moves progressively outward. At $\log(L/L_\odot) \simeq -2.9$, the outer edge of the mantle is located at $r/R \simeq 0.65$ and the inner edge at $\simeq$0.4. At this moment, the outer edge moves abruptly outward and when $\log(L/L_\odot) \simeq -3.1$ it almost reaches the surface, while the inner edge continues its progression at a slower pace. The main difference with the 0.6 $M_\odot$ white dwarf is that in this case the outer radius stabilizes at $r/R \simeq 0.9$. Finally, in both cases, the convective region disappears at about $\log(L/L_\odot) \simeq -4.5$.

The density contrast between the carbon-enriched material and the ambient liquid mixture is $\delta\rho/\rho \sim 10^{-3}$, leading to effective accelerations $a_{\rm eff} = g(\delta\rho/\rho) \simeq 2 \times 10^6$ cm s^{-2}. However, since the viscosity of Coulomb plasmas is very small, drag cannot be neglected and results in a limiting velocity of the turbulent eddies, $v_s = \sqrt{(3/8) C_b a_{\rm eff} D_b}$, where D_b is the radius of the bubble, and $C_b \approx 0.2$ in the spherical case (García-Senz & Woosley 1995). The value of D_b is not yet known, but it cannot be larger than the curvature radius at the edge of the crystallized core. When the same value found for the Earth is adopted $D_b \sim 0.1 R_{\rm core}$ (Moffatt & Loper 1994), we obtain velocities of $\sim$35 km s^{-1}.

For the thermodynamical conditions found in white dwarf interiors, viscosities are very small and conductivities rather high (Nandkumar & Pethick 1984). In particular, for the heavier white dwarf, the electrical conductivity is $\sigma = 1.3 \times 10^{21}$ s^{-1}, the magnetic diffusivity is $\eta = 5.6 \times 10^{-2}$ cm^2 s^{-1} and the kinematic viscosity is $\nu = 3.13 \times 10^{-2}$ cm^2 s^{-1}. Adopting $\sim 2 \times 10^8$ cm for the characteristic size of the convective mantle (see Figure 1, upper panel), the Reynolds and magnetic Reynolds numbers[5] range from $\sim 10^{14}$ to 10^{15}, and the magnetic Prandtl number is $\approx$0.58. Furthermore, the characteristic Ohmic decay time $\tau_\Omega \sim R_{\rm WD}^2/\eta \simeq 10^{18}$ s is much longer than the age of the white dwarf. Consequently, once the magnetic field is generated, it will remain almost constant for long times (Cumming 2002).

The aim of dynamo scaling theories is to explain the intensity of magnetic fields in terms of the properties of the region hosting the dynamo. The most comprehensive of these theories takes into account the balance between the ohmic dissipation and the energy flux available to the dynamo (Christensen 2010). The magnetic fields of the Earth and Jupiter are generated by convective dynamos powered by the cooling and chemical segregation of their interiors and it has been shown that the scaling law based on the energy fluxes can be extended to fully convective stars like T Tauri and rapidly rotating M dwarfs (Christensen et al. 2009). Therefore, it is natural to use these theories to compute the magnetic field produced by the convective mantle of crystallizing white dwarfs.

If the dynamo is saturated, the magnetic Reynolds number is large enough, and convection is described by the mixing length formalism, this scaling law can be written as (Christensen 2010)

$$\frac{B^2}{2\mu_0} = c f_\Omega \frac{1}{V} \int_{r_i}^{r_o} \left[\frac{q_c(r)\lambda(r)}{H(r)} \right]^{2/3} \rho(r)^{1/3} 4\pi r^2 dr, \qquad (1)$$

where the integral is the energy of the convective mantle, E; c is an adjustable parameter; μ_0 is the vacuum permeability; $f_\Omega \leqslant 1$ is the ratio of the Ohmic dissipation to the total dissipation; q_c is the convected energy flux; H is the scale height (temperature and compositional); V is the volume of the convective region; r_o and r_i are its outer and inner radii; and λ is the mixing length (the minimum between the density scale height and the size of the convective zone, r_o–r_i). Here, we adopt $f_\Omega = 1$ and $\lambda = H$. Also, we use the BasTI cooling sequences (Salaris et al. 2010), which, in addition to the release of latent heat, consider the energy released by chemical differentiation (Mochkovitch 1983; Segretain et al. 1994).

[5] The magnetic Reynolds number, Rm = ul/η, where u and l are typical velocities and lengths and η is the magnetic diffusivity, measures the relative importance of induction versus dissipation, while the magnetic Prandtl number is the ratio between the magnetic and the ordinary Reynolds numbers, Pm = Rm/Re.

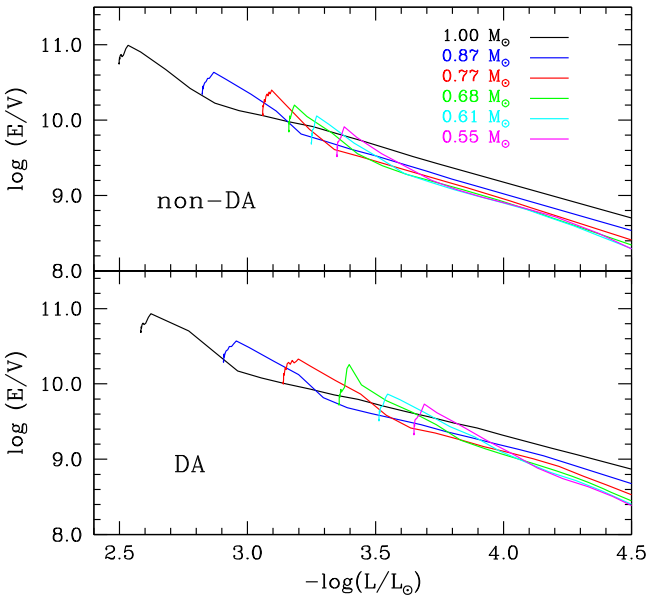

Figure 2. Convective energy density available for the dynamo as a function of the luminosity, for white dwarfs of masses 1.00, 0.87, 0.77, 0.68, 0.61, and 0.55 $M_{\odot}$. The top panel corresponds to white dwarfs with H-deficient atmospheres (non-DA), while the bottom one corresponds to stars with H-rich atmospheres (DA).

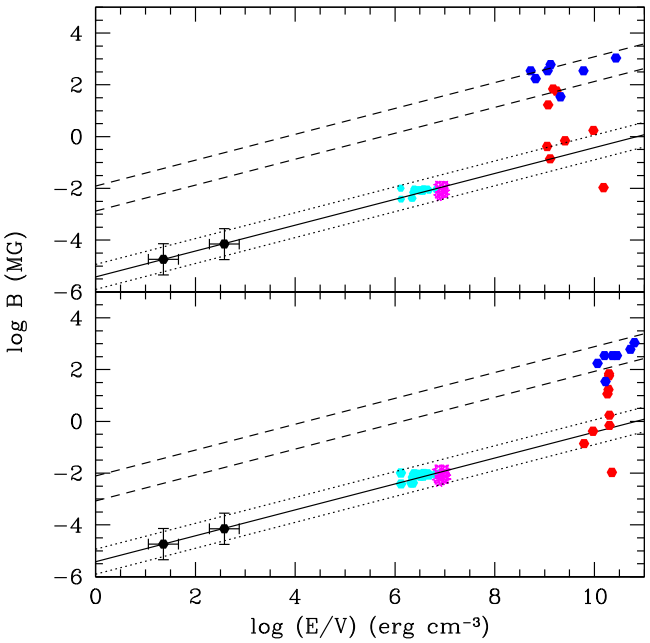

Figure 3. Magnetic field intensity as a function of the dynamo energy density. Earth and Jupiter are represented using black symbols with their corresponding error bars. T Tauri and M dwarfs are shown using cyan and magenta symbols, respectively (Christensen et al. 2009). The DA and non-DA white dwarfs listed in Table 1 are plotted as red and blue symbols, respectively. The solid line is the relationship relating the magnetic fields of the Earth, Jupiter, T Tauri, and M dwarf stars, while dotted lines allow for an additional deviation of a factor of 3 from it. The dashed lines help to represent where non-DA stars cluster. The top and the bottom panels display, respectively, the intensity of the magnetic field as a function of the present and of the maximum energy densities of the dynamo.

3. Results and Discussion

Figure 2 displays the density of convective energy available to the dynamo, namely, the r.h.s. of Equation (1) excluding the factor cf_{Ω}, for several white dwarf masses. The dynamo starts when solidification sets in, then reaches a maximum and, finally, slowly declines as the bottom of the convective mantle moves outward at fainter luminosities. This is the result of two effects. First is the mass of the star that determines when crystallization starts. White dwarfs with larger masses crystallize at larger luminosities because their central densities are also larger. The luminosity of the star also plays a role, since it determines the rate at which crystallization takes place. This luminosity, in turn, depends on the transparency of the atmosphere and the temperature of the core. The maximum energy available to the dynamo ranges from $\log E = 8.2$ to 9.6 and from 8.3 to 9.7 (c.g.s. units) for DA and non-DA white dwarfs, respectively, when masses ranging from 0.54 to 1.00 $M_{\odot}$ are considered. The scaling law relating the magnetic fields of the Earth, Jupiter, T Tauri, and M dwarf stars can be approximated by $\log B = 0.5 \log E - 5.42$—see Figure 3, solid line—and predicts that the maximum field that can be generated at the top of the dynamo range from ∼0.05 to 0.25 MG.

The X-ray emission of stars with convective regions correlates with the rotation period and with magnetic activity. The existence of a plateau in the relationship linking magnetic activity and X-ray luminosity suggests that dynamos saturate when the Rossby number $\mathrm{Ro} = P_{\mathrm{rot}}/\tau < 0.1$, τ being the convective turnover time (Wright et al. 2011; Wright & Drake 2016). For a star of mass 1.0 $M_{\odot}$, and adopting the typical values found in Section 2, the turnover time is ∼90 s. Since the critical stability rotation period is ∼6 s, we conclude that rapidly rotating white dwarfs can have saturated dynamos. Because white dwarf spectral lines are broad, measuring the rotation periods is a difficult task, and they have only been measured in pulsating and magnetic white dwarfs. Thus, their distribution of angular velocities is not well determined. Observations indicate that white dwarfs are slow rotators, but, strictly speaking, the existence of rapidly rotating white dwarfs cannot be discarded (Kawaler 2015). Within our scenario, white dwarfs with high magnetic fields would rotate rapidly and have saturated dynamos, while stars with weak fields would rotate slowly and have non-saturated dynamos. Therefore, our mechanism could easily explain white dwarfs with magnetic fields $B \lesssim 0.1$ MG.

Table 1 shows the properties of white dwarfs with carbon–oxygen cores within 20 pc of the Sun (Kawka et al. 2007; Giammichele et al. 2012). We list the name of the star, the spectral type, the magnetic field, the rotation period in hours, the mass and luminosity in solar units, the relative mass of the crystallized core and the properties of the convective mantle (the density at the inner edge, the size, and the flux at the top, all in c.g.s. units). It is important to realize that all of them, except WD 0413−077 (40 Eri B) and WD 2105−820 (L24-52), have crystallized cores. For each of these stars we computed the energy density available to the dynamo according to Equation (1) employing the value of c derived using the scaling law for the Earth and Jupiter, T Tauri stars, and M dwarfs. In the top panel of Figure 3, we show the set of calculations in which the energy density of the dynamo has been computed adopting the actual size of the convective mantle corresponding to the observed luminosity of the star, whereas in the bottom panel we show the magnetic field strength when the maximum energy density of the dynamo shown in Figure 2 is adopted. This is a reasonable assumption given the very long ohmic decay timescale. In both cases, to

Table 1
Properties of Magnetic White Dwarfs within 20 pc of the Sun

Name	Type	B (MG)	Period (hr)	$M(M_\odot)$	$\log(L/L_\odot)$	M_s/M_{WD}	ρ_b	$r_o - r_i$	q_{top}
WD 0009+501	DA	0.2	2–20	0.73 ± 0.04	-3.72	0.43	3.0×10^6	2.3×10^8	7.1×10^{10}
WD 0011−134	DA	16.7 ± 0.6	⋯	0.72 ± 0.07	-3.85	0.52	2.3×10^6	2.6×10^8	5.7×10^{10}
WD 0322−019	DA	0.120	⋯	0.63 ± 0.05	-4.02	0.52	1.6×10^6	5.2×10^8	3.0×10^{10}
WD 0413−077	DA	0.0023 ± 0.0007	⋯	0.59 ± 0.03	-1.85	0.00	⋯	⋯	⋯
WD 0548−001	non-DA	∼10	4.117	0.69 ± 0.03	-3.80	0.82	7.0×10^5	1.2×10^8	6.5×10^{10}
WD 0553+053	DA	20 ± 3	0.97	0.72 ± 0.03	-3.91	0.35	1.9×10^6	2.5×10^8	4.6×10^{10}
WD 0728+642	DA	0.0396 ± 0.0116	⋯	0.58 ± 0.00	-4.00	0.36	1.5×10^6	2.0×10^8	3.7×10^{10}
WD 0912+536	non-DA	∼100	31.9224	0.75 ± 0.02	-3.57	0.71	1.5×10^6	1.6×10^8	1.1×10^{11}
WD 1008+290	non-DA	∼100	⋯	0.68 ± 0.01	-4.31	0.93	9.8×10^4	3.0×10^6	2.1×10^{10}
WD 1036−204	non-DA	50	636 ± 36	0.60 ± 0.01	-4.19	0.76	1.9×10^5	1.1×10^7	2.5×10^{10}
WD 1309+853	DA	4.9 ± 0.5	⋯	0.71 ± 0.02	-4.01	0.60	1.6×10^6	2.3×10^8	3.4×10^{10}
WD 1748+708	non-DA	$\gtrsim$100	$\gtrsim 1.7 \times 10^4$	0.79 ± 0.01	-4.07	0.79	2.0×10^5	4.5×10^6	4.6×10^{10}
WD 1829+547	non-DA	170–180	⋯	0.90 ± 0.07	-3.94	0.85	2.7×10^5	7.2×10^6	8.3×10^{10}
WD 1900+705	non-DA	320 ± 20	$\gtrsim 8.5 \times 10^5$	0.93 ± 0.02	-2.88	0.18	1.4×10^7	2.4×10^8	1.2×10^{12}
WD 1953−011	DA	0.1–0.5	34.60224	0.73 ± 0.03	-3.38	0.13	5.6×10^6	2.4×10^8	3.3×10^{11}
WD 2105−820	DA	0.010 ± 0.001	⋯	0.74 ± 0.13	-2.93	0.00	⋯	⋯	⋯
WD 2359−434	DA	0.0031 ± 0.0005	⋯	0.78 ± 0.03	-3.26	0.12	7.2×10^6	1.8×10^8	7.3×10^{11}

Note. Data obtained from Kawka et al. (2007), Giammichele et al. (2012), and references therein.

relate the outer and inner magnetic fields we used the prescription of Christensen et al. (2009). The distribution of magnetic field strengths is clearly bimodal. Most DA white dwarfs cluster around the scaling law (the solid line in Figure 3), while non-DA white dwarfs have magnetic fields larger than DA stars with similar energy density of the dynamos. This points toward a different origin of the dynamo and/or to other scaling laws like the Coriolis-Inertial-Archimedian balance or the Magnetic–Archimedian–Coriolis balance (Christensen 2010) because the mixing length scaling law considered here demands $\sim 10^{15}$ erg s^{-1} to produce fields of ∼100 MG.

It is important to realize that the time necessary for the magnetic field to diffuse through the radiative outer layers is very long, and only the convective mantle of massive white dwarfs is close to the surface, as clearly shown in Figure 1. The final magnetic field strength will depend on how this mantle interacts with the convective envelope of cool white dwarfs. Furthermore, only white dwarfs with progenitors more massive than 2.3 $M_\odot$ can have rotation periods of minutes (Kawaler 2015). This, together with the fact that the energy of the dynamo induced by crystallization is larger for massive white dwarfs, could naturally explain why magnetic white dwarfs are more massive than average. This scenario could also explain why magnetic white dwarfs are preferentially cool. Moreover, it is likely that low-mass white dwarfs would have weaker magnetic fields confined in their interiors. Therefore, this scenario puts forward a tantalizing possibility, namely, that the magnetic fields observed in planets, non-evolved stars and white dwarfs share a common physical origin. In summary, our calculations indicate that the magnetic field observed in a sizable fraction of all white dwarfs could be the result of a dynamo generated by phase separation upon crystallization.

Furthermore, our scenario does not preclude other possibilities, but instead alleviates one of the main drawbacks of the current hypotheses to explain magnetic white dwarfs, since both the fossil field model and the binary scenario predict an insufficient number of magnetic white dwarfs. For instance, it has been long suspected that at least a fraction of high-field magnetic white dwarfs could originate from the merger of two white dwarfs (Wickramasinghe & Ferrario 2000). During the merger, a hot, differentially rotating, convective corona forms. The temperatures reached during the coalescence are so high that hydrogen is burned during the early phases of the merger. This corona is prone to magnetorotational instability, and it has been shown that can produce magnetic fields with the energy required to explain the magnetic fields of non-DA stars shown in Figure 3 (García-Berro et al. 2012). This could explain why many white dwarfs with very high magnetic fields are H-deficient. In this case, a dynamo of a completely different nature would be operating.

This work has been supported by MINECO grants ESP2013-47637-P, ESP2015-66134-R (J.I.), and AYA2014-59084-P (E.G.-B.), by the European Union FEDER funds, by grants 2014SGR1458 (J.I.), 2014SGR0038 (E.G.-B.) of the AGAUR, and by the CERCS program of the Generalitat de Catalunya.

References

Althaus, L. G., Córsico, A. H., Isern, J., & García-Berro, E. 2010, A&ARv, 18, 471
Angel, J. R. P., Borra, E. F., & Landstreet, J. D. 1981, ApJS, 45, 457
Bildsten, L., & Hall, D. M. 2001, ApJL, 549, L219
Bravo, E., Isern, J., Canal, R., & Labay, J. 1992, A&A, 257, 534
Camisassa, M. E., Althaus, L. G., Córsico, A. H., et al. 2016, ApJ, 823, 158
Christensen, U. R. 2010, SSRv, 152, 565
Christensen, U. R., Holzwarth, V., & Reiners, A. 2009, Natur, 457, 167
Cumming, A. 2002, MNRAS, 333, 589
Ferrario, L., de Martino, D., & Gänsicke, B. T. 2015, SSRv, 191, 111
Fontaine, G., Thomas, J. H., & Van Horn, H. M. 1973, ApJ, 184, 911
García-Berro, E., Lorén-Aguilar, P., Aznar-Siguán, G., et al. 2012, ApJ, 749, 25
García-Berro, E., Torres, S., Altahus, L. G., et al. 2010, Natur, 465, 194
García-Senz, D., & Woosley, S. E. 1995, ApJ, 454, 895
Giammichele, N., Bergeron, P., & Dufour, P. 2012, ApJS, 199, 29
Hollands, M. A., Gansicke, B. T., & Koester, D. 2015, MNRAS, 450, 681
Horowitz, C. J., Schneider, A. S., & Berry, D. K. 2010, PhRvL, 104, 231101
Isern, J., García-Berro, E., Hernanz, M., & Chabrier, G. 2000, ApJ, 528, 397
Isern, J., Mochkovitch, R., García-Berro, E., & Hernanz, M. 1997, ApJ, 485, 308
Kawaler, S. D. 2015, in ASP Conf. Ser. 493, 19th European Workshop on White Dwarfs, ed. P. Dufour, P. Bergeron, & G. Fontaine (San Francisco, CA: ASP), 65
Kawka, A., & Vennes, S. 2012, A&A, 538, 13
Kawka, A., & Vennes, S. 2014, MNRAS, 439, L90

Kawka, A., Vennes, S., Schmidt, G. O., et al. 2007, ApJ, 654, 499
Kepler, S. O., Pelisoli, I., Jordan, S., et al. 2013, MNRAS, 429, 2934
Kepler, S. O., Pelisoli, I., Koester, D., et al. 2016, MNRAS, 455, 3413
Koester, D., Girven, J., Gänsicke, B., et al. 2011, A&A, 530, 114
Levy, E. H., & Rose, W. K. 1974, ApJ, 193, 419
Liebert, J., Bergeron, P., & Holberg, J. 2003, AJ, 125, 348
Lister, J. R., & Buffet, B. A. 1995, PEPI, 91, 17
Mochkovitch, R. 1983, A&A, 122, 212
Moffatt, H. K., & Loper, D. E. 1994, GeoJI, 117, 394
Nandkumar, R., & Pethick, C. J. 1984, MNRAS, 209, 511
Nordhaus, J., Wellons, S., Spiegel, D. S., Metzger, B. D., & Blackman, E. G. 2011, PNAS, 108, 3135
Salaris, M., Cassisi, S., Pietrinferni, A., Kowalski, P. M., & Isern, J. 2010, ApJ, 716, 1241
Segretain, L., & Chabrier, G. 1993, A&A, 271, L13
Segretain, L., Chabrier, G., Hernanz, M., et al. 1994, ApJ, 434, 641
Sion, E. M., Holberg, J. B., Oswalt, T. D., et al. 2014, AJ, 147, 129
Tout, C. A., Wickramasinghe, D. T., Liebert, J., Ferrario, L., & Pringle, J. E. 2008, MNRAS, 387, 897
Tremblay, P. E., Fontaine, G., Freytag, B., et al. 2015, ApJ, 812, 19
Valyavin, G., & Fabrika, S. 1999, in ASP Conf. Ser. 169, 11th European Workshop on White Dwarfs, ed. S.-E. Solheim & E. G. Meistas (San Francisco, CA: ASP), 206
Valyavin, G., Shulyak, D., Wade, G. A., et al. 2014, Natur, 515, 88
Wickramasinghe, D. T., & Ferrario, L. 2000, PASP, 112, 873
Wickramasinghe, D. T., & Ferrario, L. 2005, MNRAS, 356, 1576
Wright, N. J., & Drake, J. J. 2016, Natur, 535, 526
Wright, N. J., Drake, J. J., Mamajek, E. E., & Henry, G. H. 2011, ApJ, 743, 48